Performance of DFT+*U* Approaches in the Study of Catalytic Materials

Marçal Capdevila-Cortada,[†] Zbigniew Łodziana,[‡] and Núria López*,[†]

[†]Institute of Chemical Research of Catalonia (ICIQ), The Barcelona Institute of Science and Technology, Av. Països Catalans, 16, 43007 Tarragona, Spain

[‡]The Henryk Niewodniczanski Institute of Nuclear Physics (IFJ-PAN) Radzikowskiego 152, 31-342 Kraków, Poland

1. INTRODUCTION

Catalytic materials are complex systems that contain different units, typically a carrier and an active phase. For many reactions, redox-active materials constitute the active phase. Active catalytic phases based on metal oxides include, but are not limited to, silver, copper, vanadium, molybdenum, iron, cobalt, and titanium oxides, and most notably ceria.[1,2] This results in variable occupations of the d or f states of the cations. Therefore, the proper energy alignment of these states is mandatory for the adequate description of the chemistry responsible for the catalytic processes. In particular, all the challenges related to energy-harvesting and storage technologies are intrinsically linked to the small energy difference between the different spin configurations, the easy transfer between them, and the correct alignment of the energy states.

The most powerful approach to describe the electronic structure is based on the use of density functional theory (DFT). This theory has reached an excellent balance in the accuracy−cost trade-off,[3,4] and the computational codes are nowadays benchmarked and stable.[5] Comparison with experiments is then based on upgrading the results of the electronic structure calculations through the use of transition-state theory, further embedding these calculated parameters in microkinetic models[3,6] and kinetic Monte Carlo codes.[7,8] However, the intrinsic errors that appear at the DFT level get amplified in the multiscale approaches and produce unrealistic rates for the catalytic process of interest.

The disappointing failure of DFT in the identification of the electronic structure of NiO (a Mott insulator with crystal field splitting effects, predicted to be a metal even at the GGA level of theory)[9] was one of the first indications that the self-interaction term (one electron interacts with itself), intrinsically present in the formulation of DFT, was the main responsible for this recurrent effect. The self-interaction error affects the electronic structure, up to the point of being qualitatively wrong (e.g., metals instead of semiconductors).[10] The problem is especially present in the systems with localized d or f orbitals, where electron self-repulsion leads to wrong occupation numbers and false alignment of the electronic levels, directly influencing the calculated chemistry of these materials when employed in the redox cycles. Although a variety of self-interaction corrections have been proposed,[11−15] the computational efficiency required for the description of catalytic processes, together with numerical stability issues, currently excludes the vast majority of these methods. In practice, the simplest concept of the Hubbard model, borrowed from condensed matter physics, is commonly used.[16] In this model, the electrons localized on d or f orbitals are subject to an additional on-site Coulomb interaction term, *U*, and site exchange term, *J*. They can be perceived as penalty functions forcing electron occupancy of particular orbitals that, for instance, improve the prediction of band gaps. When doing so, the electrons are more localized instead of being shared by several atoms,[17] thus breaking symmetries in local configurations and generating polarons that for some materials can be mobile at low temperatures.[18] The additional advantage of the DFT+*U* methodology is the easy implementation of energy derivatives (i.e., forces), crucial to study chemical reactions on surfaces.

Although the physical meaning of the *U* parameter might seem straightforward, it has been usually selected in an arbitrary manner,[19] fitting it to a particular problem in such a way that the experimental properties are correctly reproduced. Typical examples of such an approach are fittings to the band gap[20] or to the thermodynamics of a particular process.[21] However, fitting to one property does not ensure that the others are correctly reproduced, and this property dependence illustrates the lack of universality of DFT+*U* approaches, contrarily to the formal DFT formulation by Hohenberg, Kohn, and Sham.[22]

Alternative methodologies, focusing on the improvement of the exchange correlation functionals, have been reviewed recently by Paier.[23] The so-called hybrid functionals are based on the combination of DFT with methodologies that contain a contribution from the exact (Hartree−Fock-like) exchange, which can at least partially mitigate the problem of electron self-interaction. Such functionals come in a variety of flavors depending on the particular fraction of the exact exchange pair selected (e.g., B3LYP, PBE0, or M05-2X), and sometimes even the fraction of the exact contribution can be taken as a variable (e.g., HSE03 or HSE06). The most common hybrid functionals for periodic boundary conditions calculations are HSE03, HSE06, and PBE0. Alternatively, the random phase approximation (RPA)[24−26] method has recently emerged as a suitable tool to improve the results from DFT and more sophisticated approaches taking Taylor expansions of the correlation kernel have recently been put forward.[27] Still, these approaches are computationally very demanding and cannot be routinely employed for models of real catalysts, except for obtaining more reliable, benchmark-like, single-point energy values.

The aim of the present viewpoint is to illustrate how DFT+*U* methodologies have been employed in the study of catalytic materials and how we are using the approach in a black box

manner. To this end, we have taken an example that has been extensively analyzed in our group.[1,28,29] We aim at warning potential users about the associated errors that are non-systematic and affect adsorption and reaction steps in different manners, depending on the chemical process taking place on the surface (acid−base vs redox). The origin of the discrepancies to hybrid methods and potential ways to mitigate the problems are discussed.

2. COMPUTATIONAL TECHNIQUES

Even though DFT can be perceived as the major computational tool for the description and prediction of heterogeneous catalytic processes, it is not free from important shortcomings. As the exact exchange correlation (xc) functional is unknown, the approximate expressions for xc fail to capture the ground-state properties of the systems where the localization of electrons is present. This is related to difficulties in recovering the many-body interactions in the electron gas.[10,30]

In heterogeneous catalysis, the active materials often present localized electrons (strongly correlated), that is, transition metal oxides. Their chemical properties are governed by the properties of the valence electrons. These electrons are localized on particular d or f orbitals, and the approximate xc functionals tend to delocalize them, overstabilizing metallic ground states. As a result, DFT might predict metallic properties of catalysts that are insulators, as mentioned before for NiO.[9]

This intrinsic problem of DFT is related to the unphysical self-interaction of electrons, that is, the charge density of an individual electron interacting with itself. This repulsive interaction induces a disproportionate delocalization of the wave functions. From this perspective, the explicit introduction of the Hartree−Fock approach (the Fock exchange term is free of self-interaction) is often used to improve the accuracy of DFT via the so-called hybrid functionals.[23,31] This usually leads to insulating ground states, although this approach is still based on single-electron description. Still, better treatment of these effects requires the improved description of electron interaction many-body terms that have been formulated in the dynamical mean field theory[32] or reduced density matrix functional theory.[33] All these approaches significantly improve the prediction of the ground-state properties of bulk materials; however, they are computationally much more intensive than standard DFT. Consequently, at present, they are not practical for the description of complex surfaces or catalytic processes.

DFT+U methods, on the other hand, have only minor computational cost compared to standard DFT. The fundamentals of the Hubbard model state that the electronic correlations associated with a few localized orbitals are responsible for the complex electronic structure. These methods are based on model Hamiltonians: the Hubbard model.[16,34−36] Within this approach, the electrons in the studied system are divided into two categories: (i) the strongly correlated ones, which are usually localized on atomic d or f orbitals, are those subject to Hubbard treatment; and (ii) the remaining electrons that are treated in the standard DFT manner.

Then the energy of the system can be written as $E_{\mathrm{DFT}+U} = E_{\mathrm{DFT}} + E_{\mathrm{Hubbard}}[n] - E_{\mathrm{DC}}[n]$, where E_{Hubbard} is related to the term of the Hubbard Hamiltonian for localized orbitals, E_{DC} is the double counting term, and E_{DFT} is the total energy of standard DFT approach within the LDA or GGA approximation. The double counting term is not uniquely defined, and the specific formulation of this term results in the particular implementation of the method: for example, the around mean field (AFM)[37] or the fully localized limit (FLL)[36] methods, the latter being more widely implemented and used.

The occupation number of localized orbitals is computed by the projection of the Kohn−Sham states on the localized basis set. The implementation of this projection is an important ingredient of the DFT+U method. For the plane wave basis set representation used for slab models in heterogeneous catalysis, the local basis sets are related to the pseudopotentials. Some simplifications are usually included in the implementation to allow efficient computations of energy derivatives, like forces on atoms. In general, the rotationally invariant implementations ensure that the occupation numbers are independent with respect to the localized atomic orbital basis set rotations.[38] The electron−electron interaction integrals of the Hubbard term can be factorized with respect to angular and radial contributions. Such factorizations involve Slater integrals F^k of the radial part of the atomic wave functions. For d electrons F^0, F^2, and F^4 are required (F^6 for f states). Within this approach, effective Coulomb and exchange terms can be computed as $U = F^0$ and $J = (F^2 + F^4)/14$. In practice, simplified formulations are used, where only the lowest Slater integrals F^0 are considered. In this formulation, it is customary to introduce an effective Coulomb interaction $U_{\mathrm{eff}} = U - J$ that incorporates the exchange correction J. This simplified DFT+U scheme can be written as[39,40]

$$E_{\mathrm{DFT}+U} = E_{\mathrm{DFT}} + \frac{1}{2}U\sum_{I}\mathrm{Tr}[n^I(1-n^I)] \tag{1}$$

where I stands for the site of the ions, and n^I corresponds to the density matrices projected on localized atoms. Unless otherwise noted, this is the method discussed throughout this work. The value of U can be then obtained by different methods.[35,41−48] For the plane wave codes, one of the most extended methodologies is the constrained DFT approach that follows the linear response (LR) theory, presented by Cococcioni and Gironcoli.[40] The idea behind this methodology is to evaluate the effect of the perturbation of the bare and screened density response functions once a perturbation is applied to the local projector. To ensure that the values are meaningful, these authors indicated that the perturbation needs to be performed in supercells with increasing size, to guarantee that the values are not affected by periodic boundary conditions.[40] It has to be noted that the U value shows an important dependence on the functional of choice (LDA vs GGA), the pseudopotential, the choice of the fitting properties (if any), or projection operators. Indeed, important differences have been found, and thus, the U term shall better be reparameterized for each computational setup.[49−52] It has been proposed that the use of a unique U value for a metal ion in different environments could lead to inaccuracies when the local electronic structure changes.[41] All these procedures to obtain the Hubbard U are particularly suited for bulk systems. For the slab models representing catalysts, the U values taken from the bulk are typically used. However, the changing local environment of the surface atoms during a chemical reaction is a potential source of errors.

An exhaustive analysis employing this methodology for cerium compounds was performed by Lu and Liu.[41] These authors illustrated that adequate U values for Ce atoms in different configurations ranging from isolated atoms and ions, to small oxide compounds or extended CeO_2 bulk and surface

Table 1. Most Typical *U* Values Suggested for Several Metal Oxides Using GGA+*U* Approaches[a]

	M^{n+}	*U* (eV)	method	reference
CeO_x				
	Ce^{3+}/Ce^{4+}	2.0	fitting experimental properties	Kresse[20]
	Ce^{3+}/Ce^{4+}	2.0−3.0	fitting experimental properties	Illas[19]
	Ce^{4+}	2.0−3.0	fitting experimental properties	Fabris[61]
	Ce^{3+}	4.5	linear response	Fabris[51]
	Ce^{4+}	5.0	band gap states	Watson[62]
	Ce^{4+}	5.13	linear response	Liu[41]
	Ce^{3+}	6.70	linear response	Liu[41]
TiO_x				
	Ti^{3+}/Ti^{4+}	2.0−3.0	fitting experimental properties and band gap states	Metiu[63]
	Ti^{4+}	3.0	fitting experimental properties	Nolan[64]
	Ti^{4+}	3.0	fitting hybrid−dft calculations	Selloni[65]
	Ti^{4+}	3.4	linear response	Mattioli[66]
	Ti^{4+}	4.2	band gap states	Watson[67]
	Ti^{3+}	4.35	fitting experimental properties	Wolverton[52]
	Ti^{4+}	4.76	fitting experimental properties	Wolverton[52]
	Ti^{4+}	4.95[b]	linear response	Kitchin[68]
	Ti^{4+}	10.0	fitting experimental properties	Dupuis[69]
CoO_x				
	Co^{2+}/Co^{3+}	3.3	fitting experimental properties	Ceder[70]
	Co^{2+}/Co^{3+}	3.52	fitting experimental properties	Nørskov[71]
	Co^{2+}	3.75	fitting experimental properties	Wolverton[52]
	Co^{3+}	4.26	fitting experimental properties	Wolverton[52]
	Co^{2+}	4.4	linear response	Selloni[72]
	Co^{4+}	4.77	fitting experimental properties	Wolverton[52]
	Co^{2+}	4.0−5.0	fitting experimental properties	Doublet[73]
	Co^{3+}	6.7	linear response	Selloni[72]
MnO_x				
	Mn^{4+}	1.0−1.6	fitting experimental properties	Cockayne[74]
	Mn^{2+}	2.98	fitting experimental properties	Wolverton[52]
	Mn^{4+}	3.19	fitting experimental properties	Wolverton[52]
	Mn^{4+}	3.0−4.0	fitting experimental properties and hybrid-dft calculations	Kresse[54]
	Mn^{3+}	4.54	fitting experimental properties	Wolverton[52]
	Mn^{4+}	6.63	linear response	Kitchin[68]
FeO_x				
	Fe^{3+}	3.0	fitting experimental properties	Rollman[75]
	Fe^{3+}	3.0	fitting experimental properties	Morgan[76]
	Fe^{2+}/Fe^{3+}	3.61	fitting experimental properties	Łodziana[77]
	Fe^{2+}/Fe^{3+}	3.7	fitting experimental properties	De Leeuw[78]
	Fe^{2+}	4.04	fitting experimental properties	Wolverton[52]
	Fe^{3+}	4.09	fitting experimental properties	Wolverton[52]
MoO_x				
	Mo^{6+}	2.0	fitting experimental properties	Metiu[79]
	Mo^{6+}	6.0	fitting hybrid−dft calculations	Asta[80]
	Mo^{6+}	6.3	fitting hybrid−dft calculations	Willock[81]
	Mo^{4+}/Mo^{6+}	8.6	fitting experimental properties	Bell[56]

[a]Commonly fitted properties are the band gap, the lattice parameter, the bulk modulus, or the ΔH of formation of the oxide. The band gap states method refers to properly localize these states within the band gap. The linear response method refers to the approach introduced by Cococcioni and Gironcoli.[40]. [b]Different functionals, pseudopotentials, and TiO_2 polymorphs lead to different values of *U*.[59]

models, presented some marked characteristics: (i) the ion charge does not significantly affect the value of *U* when properly screened by counterions (*U* values for Ce atoms, Ce in $Ce_3H_xO_7$ clusters, or CeO_2 were ranging in the 4.1−5.2 eV range); and (ii) when ions are isolated the values are much larger (close to 15 and 18 eV for $Ce^{2.5+}$ and $Ce^{3.5+}$, respectively). Thus, the environment and its polarizability turn out to be crucial to screen the Coulomb interactions on Ce 4f orbitals effectively. This observation agrees with Cococcioni and Gironcoli,[40] who found that to obtain Ce 4f values, on-site and nearest neighbors interactions are needed for Ce in its metallic form.[53]

An extensive compilation of *U* values for Co, Fe, Ni, Cr, Mn, V, and Ti ions on different oxide and fluoride environments has been presented by Aykol and Wolverton on the basis of the experimental ΔH of formation fitting approach.[52] These authors aimed at reproducing accurate thermochemistry,[54,55] making special emphasis on the role of the oxidation state and ligand contributions. They observed, for instance, that the *U* term is not transferable when going from oxygen to fluoride

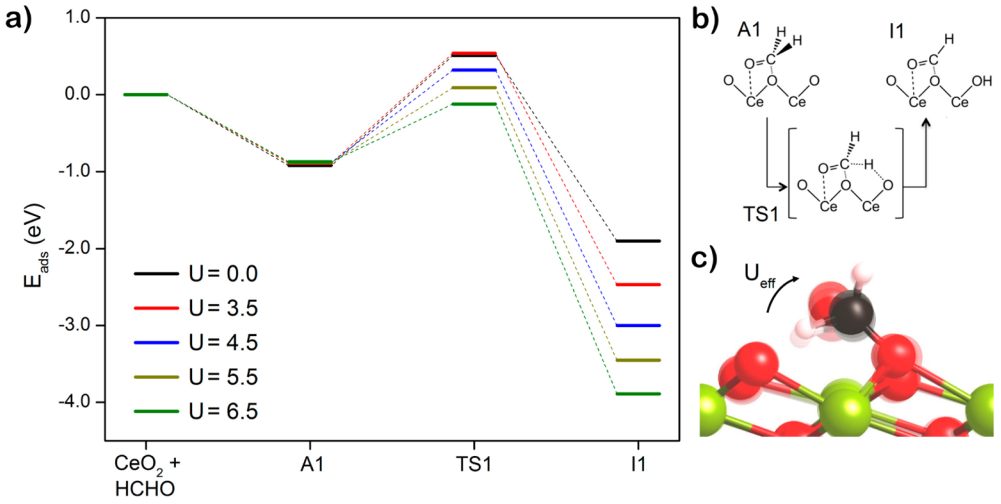

Figure 1. (a) Adsorption of formaldehyde (A1) on the CeO_2(111) regular surface and first hydrogen stripping to CHO and OH (I1). (b) Reaction scheme for this elementary step. (c) Overlaid structures of TS1 for the different *U* values. Red stands for oxygen, yellow for cerium, black carbon, and white hydrogen.

ligands, and is larger when the charge of the cation increases (although exceptions are identified). Similarly, Bell and co-workers,[56] when investigating the reduction energies for transition (Ti, V, Mo) and rare earth (Ce) metal oxides, observed that the value of *U* had to be adjusted for each reaction. The same authors in the investigation of the reducible transition metal oxides, basically $Bi_2Mo_3O_{12}$ for hydrogen abstraction from propene, observed that both the barrier and the final state energy depend on the *U* parameter used for Mo.[57] When compared to their reference functional, M06-L,[58] the thermodynamic and the kinetic parameters were not reproduced with a single *U* value. In a similar study that focused on the structure of different TiO_2 polymorphs, Kitchin et al. realized that the *U* value obtained by linear response for the Ti d orbitals depends on the functional and pseudopotential employed, and the particular crystal structure.[59] Similar conclusions were obtained by Greeley et al. for several transition-metal (hydroxy)oxides, where the dependence of the enthalpy of formation with the *U* term varies significantly when van der Waals effects were considered.[60]

In Table 1 we present a summary of the most common *U* values employed together with the GGA formulation. These values can range from 2.0 to 10.0 eV for TiO_x or from 2.0 to 8.6 eV for MoO_x, depending on a variety of factors.

In the present work, we have employed PBE+*U* with variable *U* values in order to unravel the robustness of the different approaches to obtain *U* and how the values affect the catalytic properties of the materials. To this end, we have used the VASP code[82,83] with the PBE functional,[84] PAW pseudopotentials,[85] and plane waves with a cutoff energy of 500 eV for the valence electrons (5s, 5p, 4f, 6s for Ce atoms, 3d, 4s for Fe, 2s, 2p for O and C, and 1s for H). The lattice parameter was optimized using a dense Γ-centered 7 × 7 × 7 k-point mesh that leads to a value of 5.497 Å, in good agreement with the experimental a_{exp} of 5.411 Å. The (111) surface, the most stable termination of ceria, was modeled as a $p(2 \times 2)$ supercell with periodically repeated slabs consisting of three O−Ce−O layers (nine single layers) separated by 15 Å of vacuum space, which was optimized using a Γ-centered (3 × 3 × 1) k-point mesh. The five outermost single layers and the adsorbate(s) were allowed to relax, whereas the rest of the atoms were kept fixed to their bulk positions. Using the same setup, screened hybrid HSE06 calculations[86] have been performed and employed as reference to illustrate the dependence of the reactivity with the different values of *U*. The iron oxide slab contains 18 atomic layers and a k-point sampling of 5 × 3 × 1 was employed.

3. DISCUSSION

3.1. Formaldehyde Decomposition on CeO_2(111).

Cerium oxide is among the most interesting oxides from a chemical point of view. The coexistence of acid−base, redox, and oxygen storage material properties makes it an outstanding ingredient in catalytic formulations where it can act as active phase, cooperative or synergetic catalytic phase, or just as support.[28,87] The hydrophobicity of the surface can also be tuned by the reduction degree.[88,89] Applications centered on its oxidative capacity have been preeminent: ceria is then usually present in combination with metal phases, although recently it has been shown to be active as a single phase in the Deacon and HBr oxidation reactions,[90,91] hydrogenations,[92−95] and selective C−C bond breaking.[96] Shape-directed synthesis protocols enable the synthesis of tailored ceria nanoparticles,[97,98] in particular, nanocubes exposing {100} facets. The latter, which are polar and present two main reconstructions,[99,100] exhibit unique catalytic activity.[93]

Many of these reactions combine acid−base and redox elementary steps. In the latter, one of the electrons from reactants and/or products can be accommodated at the surface cations. Therefore, the correct identification of the energy gain/loss by the reductive nature of the cations on the surface constitutes a major issue. To illustrate the effect, we have taken as an example the dissociation of formaldehyde on the ceria (111) surface, for which detailed temperature program desorption experiments exist.[101−103] The elementary step for dehydrogenation of formaldehyde is found in Figure 1.

The most common values of *U* for LDA and PBE functionals are 5.3 and 4.5 eV,[51] which have been extensively used in the literature. The results of the reaction energy profiles obtained with PBE+*U* for different values of *U* are intriguing (Figure 1). Formaldehyde adsorption remains constant, as it does not involve any surface reduction, and thus, all points (CH_2O + * → CH_2O*) lie in the same energy. In contrast, the elementary

step for the decomposition of formaldehyde ($CH_2O^* \rightarrow CHO^* + H^*$) is always exothermic, but the energy span between the small and large U values is more than 2 eV. The reaction is more exothermic as the U increases. A similar behavior was observed by Bennett and Jones for CO+NO reaction on the ceria surface.[104] More importantly, the energy of the transition state also presents a wide range of values that expands about 1 eV. Considering that the computed activation energy is introduced in the exponential in the transition-state theory, this means that at room temperature the difference in the kinetic coefficient for small and large values of U on Ce can account for several orders of magnitude.

A clearer view of the process can be noticed when the adsorption-, transition-, and final-state energies are included in the same plot, see Figure 2. The figure clearly illustrates that the balance between thermodynamics and kinetics is broken. The kinetics of the system are wrong for several U values, and the energy of the transition state with respect to the gas-phase reference changes from positive to negative depending on the strength of the effective U parameter. In Figure 2, the problem of electronic structure and how it is dealt with in DFT+U approaches becomes clear. While formaldehyde adsorption is a constant and thus is not affected by changes in the U parameter, the following step in the decomposition is strongly affected. For small U values, the electrons are still delocalized, and thus, the values for the transition and final states are rather constant. For higher values of U, the adsorption remains constant, but the transition and final states reduce their energies according to a linear dependence, yet with different slopes.

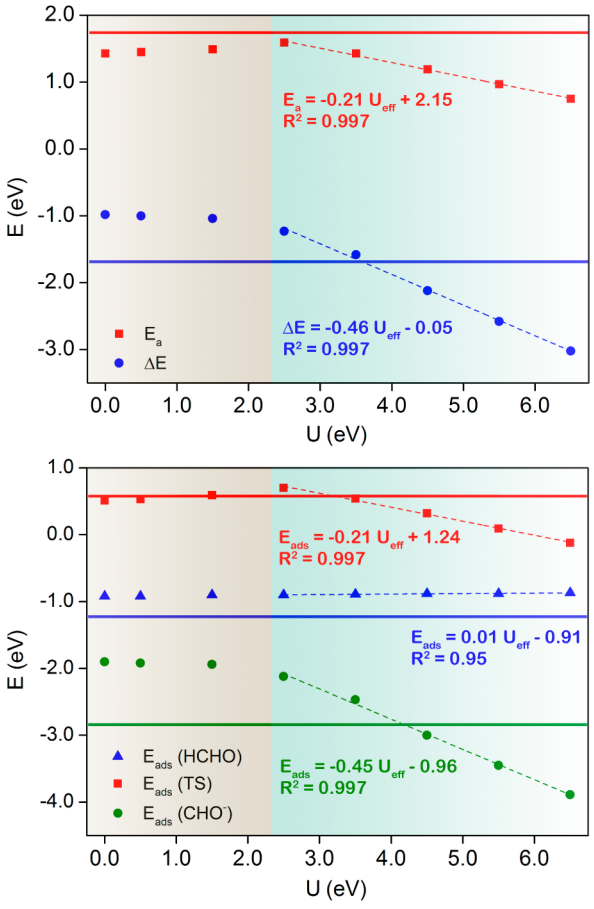

Figure 2. (Top) Activation energy (E_a, red) and reaction energy (ΔE, blue) for the first C−H bond breaking of formaldehyde on CeO_2(111) as a function of the U parameter. (Bottom) Adsorption energy of formaldehyde (blue), transition step for first hydrogen striping (red), and final state (green), all with respect to gas-phase formaldehyde and the bare CeO_2(111) surface, as a function of U. In both cases, the horizontal lines account for the screened hybrid HSE06 results. PBE0 calculations provide nearly identical results as HSE06 (see text). For the redox processes, dependence on the U parameter is observed when electron localization in the Ce centers appears (turquoise background color). Notably, the dependences of the kinetic and thermodynamic terms are different.

At small U values, electrons are not localized even in reduced surface conditions, and thus, for U values lower than a certain threshold (that depends on the material), all the energy parameters for adsorption, transition, and thermodynamics of the elementary steps are practically constant. Instead, at medium to large U values, both the transition and final states are stabilized, but the size of this stabilization is doubled for the final state. This means that the thermodynamics and the kinetics are no longer synchronous, and the choice of U implies an error in one or the other. Comparison with experiments for formaldehyde decomposition sets an experimental constraint to the transition-state energy, as it should be larger than zero to explain that desorption is preferred when compared to dehydrogenation.[102,103] This only happens for U values below 5.5 eV, thus constituting the upper bound to this parameter.

The influence of the U parameter on the direct reducibility of the surface has also been assessed (Figure 3). This reducibility,

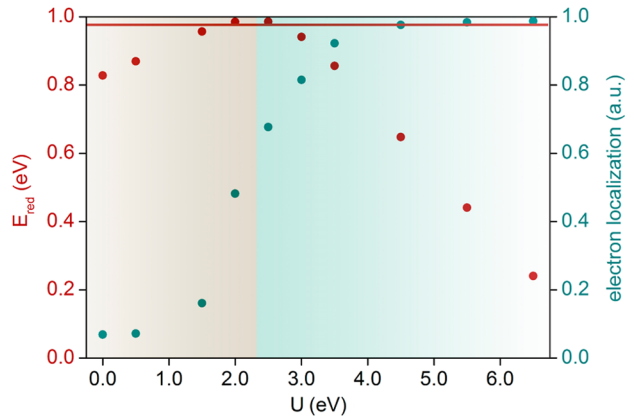

Figure 3. Reduction energy (E_{red}, red) and electron localization (turquoise) as a function of the Hubbard U parameter. The horizontal solid line accounts for the screened hybrid HSE06 E_{red} result. The background color indicates when the electron is properly localized in the Ce center (turquoise).

E_{red}, has been taken as the energy difference between the $p(2 \times 2)$ supercell with one extra electron added (where a background charge is added to preserve charge neutrality) and the bare $p(2 \times 2)$ surface, as considered in previous work.[1,28] The electron localization on a single cerium atom of the topmost layer is also shown in Figure 3, for each value of U.

The interpretation of the dependence with the U term in the redox steps and the difference between the kinetics and thermodynamics can be traced back to the local structures and the electronic states of these configurations. The different slopes observed for the reaction and transition-state energies with the U parameter originate from the number of electrons that are localized at the surface. The ratio between the slopes gives the ratio between the electrons at the surface.

When compared to more accurate screened hybrid calculations (HSE06), the U values at which the agreement is obtained vary for the kinetic and the thermodynamic parameters (solid lines in Figure 2). This means that to match the HSE06 results a value of 4.27 eV is required for the thermodynamics of the process, but only of 3.33 eV for the transition state. Similarly, hybrid PBE0 calculations provided almost identical results (4.32 and 3.33 eV, respectively). The calculation of E_{red}, Figure 3, where one electron was added to the bare surface slab (comparable then with the previous HCHO transition-state calculation), leads to a U value of 2.58 eV to reproduce the HSE06 result. Indeed, Kulik and Marzari[105] reported that the complete potential-energy surface cannot be represented by a constant U value, through the study of the dissociation of $^4\Phi$ FeO^+ by internuclear separation. Instead they proposed that the geometry plays a major role and that, rather than being a parameter, U is a function of the local geometry. It is worth stressing that although the HSE06 functional also contains certain degree of inaccuracy, it typically outperforms LDA(+U) and GGA(+U), especially for the description of semiconductor and insulator materials.[23,106−109] Thus, hybrid functional results should not be considered as the gold standard but rather as a higher rung in Jacob's ladder of DFT. Proper benchmark studies should be performed using more accurate RPA or QMC calculations, but these are beyond the scope of this work.

The origin of the different U to fit the HSE06 values thus can be traced back to the local structures. For ceria, Lu and Liu[41] identified the dependence of the U parameter on the geometry of the environment: the larger the Ce−O distance, the larger the oxygen screening loss, and thus, the larger the interaction of the f electrons shall be (i.e., larger U). These authors illustrated that for variations of 0.1 Å, the effect on the U could be as large as about 0.4 eV. We have compared the elastic modifications both for the transition and final states at a given U = 3.5 eV, Figure 4.

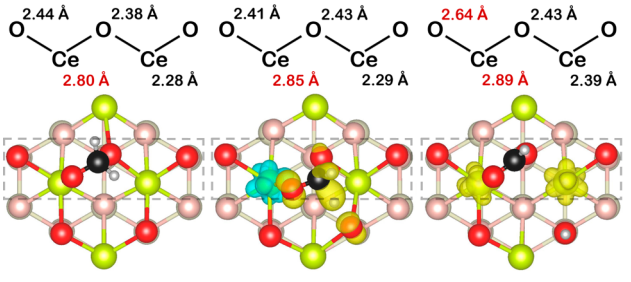

Figure 4. (Top) Most relevant Ce−O distances in Å for the initial, transition, and final states of formaldehyde decomposition on CeO_2 at PBE+U (U = 3.5 eV) level. (Bottom) Electron localization in the initial, transition, and final states. Same color code as in Figure 1.

In contrast, acid−base steps do not present this problem. We have performed the first reaction in methanol decomposition on ceria(110), in the same manner as presented before. The adsorption, transition, and final states (i.e., the thermodynamics and kinetics) are completely stable and completely independent of the U parameter. This seems to be a reasonable conclusion because no surface atoms are reduced during the process. However, it sets an internal contradiction to generate reaction energy profiles that maintain the correct balance of the kinetics and thermodynamics in complex reaction networks that contain both acid−base and redox steps.

The structurally consistent U suggested by Kulik and Marzari is at the origin of the problem. These authors observed the need for a smooth potential energy curve incorporating the variations of U (structurally consistent U) when the significant changes in the hybridization and occupancy of a transition-metal center occur along the reaction coordinate. When the authors introduced a polyatomic molecular system, they recognized that more than one geometric variable affects the occupation matrix of the d-states and thus the U term depends on several variables, $U(\boldsymbol{R})$. Other structurally consistent approaches were also indicated in the literature, and the effect when changing the coordination by adsorption of different O-containing species was reported for Ti.[68,110] Kulik and Marzari proposed CCSD(T) calculations as an appropriate benchmark and suggested that the inclusion of a $U(\boldsymbol{R})$ in the nudged elastic band is "trivial". However, five years after this comment, we are not aware of such implementation. Unfortunately, although this approach seems evident, it could only be applied to very small systems (with one metal atom) that did not present a set of close-lying states.

Indeed, the search of transition-state calculations with DFT and plane waves codes has an important problem when dealing with the electronic structure. The reason is that in the algorithms to search for transition states, the files that describe the electronic structure are taken to be the same (i.e., the U for each of the configurations along the band is identical). As we have seen before, the strength of the U parameter seems to provide unreasonable values for the kinetics. We propose here a methodology that can smooth the errors: (i) to identify acid−base and redox steps; (ii) to determine of the most adequate U value by comparison of the thermodynamics of the steps to a reference calculation (ideally RPA or QMC, otherwise hybrid DFT); (iii) to unravel the dependence of the thermodynamics with the U (as in Figure 2); (iv) to elaborate on the kinetics an accurate count of the electron localization at the transition state and comparison to its corresponding final state is needed, as this gives the slope for the dependence of the transition state with U; and (v) to rescale the U value for the transition state according to the geometric perturbation between transition and final states. This procedure is more stable than employing variable U for each initial image in the band, as the initial guesses both in terms of electronic structure and geometry might significantly differ from the final solution. This is possible because, at a difference from molecular calculations, many of these steps correspond to bound initial and final states.

3.2. Iron Oxides. Iron oxides are among the cheapest catalysts and present a very versatile structure that accommodates different oxygen stoichiometries. The structure of the material presents certain difficulties in the adequate description of its electronic structure that are linked to the metal−insulator transition occurring in some of its phases (Verwey transition).[77] The use of U, applied to the Fe 3d orbitals, is crucial to obtain a proper orbital ordering to understand surface reconstructions in a material as common as Fe_3O_4. In that case, the U value employed was 3.61 eV.[77] For a completely different stoichiometry, in the study of water interacting with iron oxide films, the effective U value was very similar, 3.0 eV. In both cases the U values were fitted for the PW91 functional and, as also observed by Lu and Liu for ceria, the charge of the cation is not the primary term affecting the U value.[41] To analyze the extension of the problem, we have investigated the same reaction ($CH_2O^* + * \rightarrow CHO^* + H^*$) on Fe_2O_3. Again, the observed patterns for adsorption, reaction energy for the

first abstraction, and the corresponding transition-state energy (Figure 5) resemble those in Figure 2. However, two

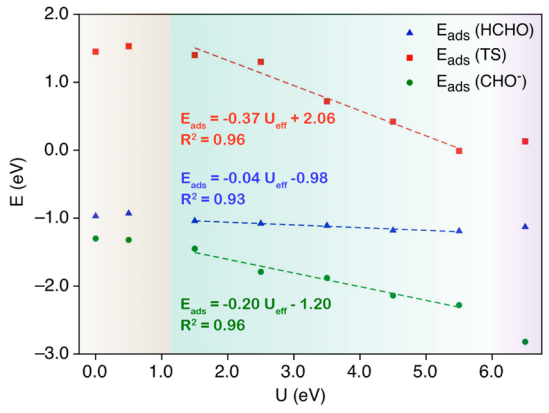

Figure 5. Adsorption energy of formaldehyde (blue), transition step for first hydrogen stripping (red), and final state (green), all with respect to gas-phase formaldehyde and the bare Fe_2O_3 surface, as a function of *U*. The background color indicates when the electron is properly localized in the Fe center (turquoise) and when spin-crossing is observed (purple). Notably, the dependences of the kinetic and thermodynamic terms are different.

remarkable points emerge. First, the dependencies are different from those in Figure 2, where now the transition-state slope is larger than that for the reaction energy. This behavior can be traced back to the occupation of the d shell versus f shell in Fe versus Ce. The former is by reduction more than half full, while that of Ce is empty or with less than one electron. Second, at high *U* values (6.5 eV, purple region of Figure 5), the electronic state of the initial and final states are not the same as for intermediate values of *U*, and therefore, the corresponding energies do not follow the trends. Yet, this highlights a problem that is much more acute for less oxidized oxides, like FeO. Our preliminary results for that surface show that spin-crossings can occur at different positions of the intrinsic reaction paths connecting reactants and products, and thus the equivalent results to those in Figure 2 and 5 will develop in families of planes for each of the spin states considered.

3.3. Complex Interfaces and Single-Atom Catalysts. The problem of different *U* values might be also acute in the case of isolated atoms or monomers. An example that parallels our investigation on methanol conversion is the same reaction on vanadyl ions and clusters supported on CeO_2.[111,112] These atoms form a complex interface for which Ce 4f *U* values were employed,[111] but then the cooperative effects (as there are two different centers that can be reduced competitively) are difficult to unravel. Therefore, identification of the active vanadium containing species might not be trivial.[112]

The case of the VO_x/CeO_2 materials shares some common features with single-atom catalysts, SAC, proposed for isolated atoms in oxide matrices. The term was coined by Zhang and co-workers[113] for the description of isolated Pt atoms embedded in FeO_x, which were tested in CO oxidation, but follows similar principles to the Au/CeO_2 or Pt/CeO_2 chemistry reported by Flytzani-Stephanopoulos.[114] In all these cases, the theoretical simulations performed to understand this chemistry have been carried out with a *U* value derived from the clean host material. For the Pt/FeO_x oxide, the authors took a $U = 3$ eV from hematite.[115] However, as we have shown, this approximation might really diverge from the optimal value, as the local geometric perturbations induced by single-atom configurations might be very large.

3.4. Other Materials Related to Energy Production and Storage. The problems observed in understanding the chemistry of ceria and iron oxides can be further extended to other materials where an adequate band alignment is needed to rationalize the chemical processes. Examples of such behavior can be found in several studies,[116−118] which illustrate that the proper band alignment in titania is required for the photoelectrochemical properties to be well-balanced, particularly in complex interfaces. The fitting of *U* for the different cations is required. Still, some authors have proposed that the use of linear response DFT+*U* in reactions, like the oxygen evolution activity on rutiles, would only change the activity ordering of different materials.[68] According to these authors, the weakening of the adsorption energies (taken as descriptors) will not affect the relative ordering of reaction energies and, at most, the variation will only affect the top of the activity volcano. In view of our results, larger differences shall be expected for doped systems,[119] particularly if chemical and electrochemical steps are present in the reaction network.[120]

The problem is also prevalent for other compounds, like cobalt oxide, with a wide range of stable compositions seem particularly difficult. Recent studies have employed the fitted values of *U* from Wang and Ceder,[70] which were adapted to reproduce thermodynamic properties (ΔH of formation of the oxide), but still corrections were needed to obtain the proper thermodynamics between the different phases.[121] Similar problems arise in manganese oxides, for which site-dependent values were proposed,[54] and the most recent use of nickel oxohydroxides[122−124] with varied valences of the Ni centers and mixed Fe−Ni materials for energy-related catalysis[125,126] are foreseen. The implication of the *U* dependence will also affect other families of materials with applications in Li-ion batteries, water splitting, or photovoltaics such as Prussian Blue analogues,[127,128] perovskites,[129,130] or Li-ion battery cathodes.[52]

4. OUTLOOK

Computational techniques based on DFT have reached a level of maturity that makes possible the accurate reproduction of experiments and the prediction of reactivity up to levels that seemed unreachable just a decade ago. The statement is particularly true for metals and insulators, but for materials with complex electronic structures, multiple spin configurations, and different degrees of electron localization, this is not so straightforward. We have shown how the thermodynamics and the kinetics for a simple reaction respond differently to the external energy penalty included in the models to account for proper representation of the band gap. The ultimate result is that the dispersion leads to a complete disagreement between the experimental observations and the computed values. In this Viewpoint, we presented a revision of what needs to be done to achieve a reasonable accuracy at a reasonable computational cost, so as to improve the use of DFT for strongly correlated systems. Most of the chemistry related to photochemistry, energy extraction to suitable energy vectors, conversion, and storage are based on the use of materials with complex electronic structures, and thus, the results here are of fundamental interest to the community.

AUTHOR INFORMATION

Corresponding Author

*E-mail: nlopez@iciq.es.

ORCID

Marçal Capdevila-Cortada: 0000-0003-4391-6580
Núria López: 0000-0001-9150-5941

Notes

The authors declare no competing financial interest.

■ ACKNOWLEDGMENTS

We thank MINECO (CTQ2015-68770-R) for financial support and BSC-RES for providing generous computer resources. M.C.-C. also acknowledges MINECO for a "Juan de la Cierva – Formación" fellowship (FJCI-2014-20568). Z.L. acknowledges NSC Poland support through project 2015/17/B/ST3/02478.

■ REFERENCES

(1) Capdevila-Cortada, M.; Vilé, G.; Teschner, D.; Pérez-Ramírez, J.; López, N. *Appl. Catal., B* **2016**, *197*, 299−312.
(2) Montini, T.; Melchionna, M.; Monai, M.; Fornasiero, P. *Chem. Rev.* **2016**, *116*, 5987−6041.
(3) Sutton, J. E.; Guo, W.; Katsoulakis, M. A.; Vlachos, D. G. *Nat. Chem.* **2016**, *8*, 331−337.
(4) Nørskov, J. K.; Bligaard, T.; Rossmeisl, J.; Christensen, C. H. *Nat. Chem.* **2009**, *1*, 37−46.
(5) Lejaeghere, K.; Bihlmayer, G.; Bjorkman, T.; Blaha, P.; Blugel, S.; Blum, V.; Caliste, D.; Castelli, I. E.; Clark, S. J.; Dal Corso, A.; de Gironcoli, S.; Deutsch, T.; Dewhurst, J. K.; Di Marco, I.; Draxl, C.; Dulak, M.; Eriksson, O.; Flores-Livas, J. A.; Garrity, K. F.; Genovese, L.; Giannozzi, P.; Giantomassi, M.; Goedecker, S.; Gonze, X.; Granas, O.; Gross, E. K. U.; Gulans, A.; Gygi, F.; Hamann, D. R.; Hasnip, P. J.; Holzwarth, N. A. W.; Iu an, D.; Jochym, D. B.; Jollet, F.; Jones, D.; Kresse, G.; Koepernik, K.; Kucukbenli, E.; Kvashnin, Y. O.; Locht, I. L. M.; Lubeck, S.; Marsman, M.; Marzari, N.; Nitzsche, U.; Nordstrom, L.; Ozaki, T.; Paulatto, L.; Pickard, C. J.; Poelmans, W.; Probert, M. I. J.; Refson, K.; Richter, M.; Rignanese, G.-M.; Saha, S.; Scheffler, M.; Schlipf, M.; Schwarz, K.; Sharma, S.; Tavazza, F.; Thunstrom, P.; Tkatchenko, A.; Torrent, M.; Vanderbilt, D.; van Setten, M. J.; Van Speybroeck, V.; Wills, J. M.; Yates, J. R.; Zhang, G.-X.; Cottenier, S. *Science* **2016**, *351*, aad3000.
(6) Teschner, D.; Novell-Leruth, G.; Farra, R.; Knop-Gericke, A.; Schlögl, R.; Szentmiklósi, L.; González Hevia, M.; Soerijanto, H.; Schomäcker, R.; Pérez-Ramírez, J.; López, N. *Nat. Chem.* **2012**, *4*, 739−745.
(7) Pogodin, S.; López, N. *ACS Catal.* **2014**, *4*, 2328−2332.
(8) Stamatakis, M.; Vlachos, D. G. *J. Chem. Phys.* **2011**, *134*, 214115.
(9) Shen, Z.-X.; List, R. S.; Dessau, D. S.; Wells, B. O.; Jepsen, O.; Arko, A. J.; Barttlet, R.; Shih, C. K.; Parmigiani, F.; Huang, J. C.; Lindberg, P. A. P. *Phys. Rev. B: Condens. Matter Mater. Phys.* **1991**, *44*, 3604−3626.
(10) Martin, R. M.; Reining, L.; Ceperley, D. M.*Interacting Electrons: Theory and Computational Approaches*; Cambridge University Press: Cambridge, U.K., 2016.
(11) Perdew, J. P.; Zunger, A. *Phys. Rev. B: Condens. Matter Mater. Phys.* **1981**, *23*, 5048−5079.
(12) Szotek, Z.; Temmerman, W. M.; Winter, H. *Phys. Rev. B: Condens. Matter Mater. Phys.* **1993**, *47*, 4029−4032.
(13) Tsuneda, T.; Hirao, K. *J. Chem. Phys.* **2014**, *140*, 18A513.
(14) Zawadzki, P.; Jacobsen, K. W.; Rossmeisl, J. *Chem. Phys. Lett.* **2011**, *506*, 42−45.
(15) Gudmundsdóttir, H.; Jónsson, E. Ö.; Jónsson, H. *New J. Phys.* **2015**, *17*, 083006.
(16) Hubbard, J. *Proc. R. Soc. London, Ser. A* **1963**, *276*, 238−257.
(17) Ganduglia-Pirovano, M.; Da Silva, J.; Sauer, J. *Phys. Rev. Lett.* **2009**, *102*, 26101.
(18) Kowalski, P. M.; Camellone, M. F.; Nair, N. N.; Meyer, B.; Marx, D. *Phys. Rev. Lett.* **2010**, *105*, 146405.
(19) Loschen, C.; Carrasco, J.; Neyman, K. M.; Illas, F. *Phys. Rev. B: Condens. Matter Mater. Phys.* **2007**, *75*, 35115.
(20) Da Silva, J. L. F.; Ganduglia-Pirovano, M. V.; Sauer, J.; Bayer, V.; Kresse, G. *Phys. Rev. B: Condens. Matter Mater. Phys.* **2007**, *75*, 45121.
(21) Nolan, M.; Parker, S. C.; Watson, G. W. *Surf. Sci.* **2005**, *595*, 223−232.
(22) Perdew, J. P.1995; pages 51−64.
(23) Paier, J. *Catal. Lett.* **2016**, *146*, 861−885.
(24) Bohm, D.; Pines, D. *Phys. Rev.* **1951**, *82*, 625−634.
(25) Pines, D.; Bohm, D. *Phys. Rev.* **1952**, *85*, 338−353.
(26) Bohm, D.; Pines, D. *Phys. Rev.* **1953**, *92*, 609−625.
(27) Erhard, J.; Bleiziffer, P.; Görling, A. *Phys. Rev. Lett.* **2016**, *117*, 143002.
(28) Capdevila-Cortada, M.; López, N. *ACS Catal.* **2015**, *5*, 6473−6480.
(29) Capdevila-Cortada, M.; García-Melchor, M.; López, N. *J. Catal.* **2015**, *327*, 58−64.
(30) Mahan, G. D.*Many-Particle Physics*; Springer U.S.: Boston, MA, 2000.
(31) Becke, A. D. *J. Chem. Phys.* **1993**, *98*, 1372.
(32) Georges, A.; Kotliar, G.; Krauth, W.; Rozenberg, M. J. *Rev. Mod. Phys.* **1996**, *68*, 13−125.
(33) Yang, W.; Zhang, Y.; Ayers, P. W. *Phys. Rev. Lett.* **2000**, *84*, 5172−5175.
(34) Gutzwiller, M. C. *Phys. Rev. Lett.* **1963**, *10*, 159−162.
(35) Anisimov, V. I.; Gunnarsson, O. *Phys. Rev. B: Condens. Matter Mater. Phys.* **1991**, *43*, 7570−7574.
(36) Anisimov, V. I.; Solovyev, I. V.; Korotin, M. A.; Czyżyk, M. T.; Sawatzky, G. A. *Phys. Rev. B: Condens. Matter Mater. Phys.* **1993**, *48*, 16929−16934.
(37) Anisimov, V. I.; Zaanen, J.; Andersen, O. K. *Phys. Rev. B: Condens. Matter Mater. Phys.* **1991**, *44*, 943−954.
(38) Liechtenstein, A. I.; Anisimov, V. I.; Zaanen, J. *Phys. Rev. B: Condens. Matter Mater. Phys.* **1995**, *52*, R5467−R5470.
(39) Dudarev, S. L.; Botton, G. A.; Savrasov, S. Y.; Humphreys, C. J.; Sutton, A. P. *Phys. Rev. B: Condens. Matter Mater. Phys.* **1998**, *57*, 1505−1509.
(40) Cococcioni, M.; de Gironcoli, S. *Phys. Rev. B: Condens. Matter Mater. Phys.* **2005**, *71*, 35105.
(41) Lu, D.; Liu, P. *J. Chem. Phys.* **2014**, *140*, 084101.
(42) Gunnarsson, O.; Andersen, O. K.; Jepsen, O.; Zaanen, J. *Phys. Rev. B: Condens. Matter Mater. Phys.* **1989**, *39*, 1708−1722.
(43) Mosey, N. J.; Carter, E. A. *Phys. Rev. B: Condens. Matter Mater. Phys.* **2007**, *76*, 155123.
(44) Mosey, N. J.; Liao, P.; Carter, E. A. *J. Chem. Phys.* **2008**, *129*, 014103.
(45) Springer, M.; Aryasetiawan, F. *Phys. Rev. B: Condens. Matter Mater. Phys.* **1998**, *57*, 4364−4368.
(46) Shih, B.-C.; Abtew, T. A.; Yuan, X.; Zhang, W.; Zhang, P. *Phys. Rev. B: Condens. Matter Mater. Phys.* **2012**, *86*, 165124.
(47) Aryasetiawan, F.; Imada, M.; Georges, A.; Kotliar, G.; Biermann, S.; Lichtenstein, A. I. *Phys. Rev. B: Condens. Matter Mater. Phys.* **2004**, *70*, 195104.
(48) Himmetoglu, B.; Floris, A.; de Gironcoli, S.; Cococcioni, M. *Int. J. Quantum Chem.* **2014**, *114*, 14−49.
(49) Fabris, S.; de Gironcoli, S.; Baroni, S.; Vicario, G.; Balducci, G. *Phys. Rev. B: Condens. Matter Mater. Phys.* **2005**, *71*, 41102.
(50) Kresse, G.; Blaha, P.; Da Silva, J. L. F.; Ganduglia-Pirovano, M. V. *Phys. Rev. B: Condens. Matter Mater. Phys.* **2005**, *72*, 237101.
(51) Fabris, S.; de Gironcoli, S.; Baroni, S.; Vicario, G.; Balducci, G. *Phys. Rev. B: Condens. Matter Mater. Phys.* **2005**, *72*, 237102.
(52) Aykol, M.; Wolverton, C. *Phys. Rev. B: Condens. Matter Mater. Phys.* **2014**, *90*, 115105.
(53) Notice that for other metals, like Fe, the same authors indicate that second-nearest-neighbors effects are also important.
(54) Franchini, C.; Podloucky, R.; Paier, J.; Marsman, M.; Kresse, G. *Phys. Rev. B: Condens. Matter Mater. Phys.* **2007**, *75*, 195128.
(55) Jain, A.; Hautier, G.; Ong, S. P.; Moore, C. J.; Fischer, C. C.; Persson, K. A.; Ceder, G. *Phys. Rev. B: Condens. Matter Mater. Phys.* **2011**, *84*, 45115.

(56) Lutfalla, S.; Shapovalov, V.; Bell, A. T. *J. Chem. Theory Comput.* **2011**, *7*, 2218−2223.
(57) Getsoian, A. "Bean"; Bell, A. T. *J. Phys. Chem. C* **2013**, *117*, 25562−25578.
(58) Zhao, Y.; Truhlar, D. G. *J. Chem. Phys.* **2006**, *125*, 194101.
(59) Curnan, M. T.; Kitchin, J. R. *J. Phys. Chem. C* **2015**, *119*, 21060−21071.
(60) Zeng, Z.; Chan, M. K. Y.; Zhao, Z.-J.; Kubal, J.; Fan, D.; Greeley, J. *J. Phys. Chem. C* **2015**, *119*, 18177−18187.
(61) Huang, M.; Fabris, S. *J. Phys. Chem. C* **2008**, *112*, 8643−8648.
(62) Nolan, M.; Grigoleit, S.; Sayle, D. C.; Parker, S. C.; Watson, G. W. *Surf. Sci.* **2005**, *576*, 217−229.
(63) Hu, Z.; Metiu, H. *J. Phys. Chem. C* **2011**, *115*, 5841−5845.
(64) Nolan, M.; Elliott, S. D.; Mulley, J. S.; Bennett, R. A.; Basham, M.; Mulheran, P. *Phys. Rev. B: Condens. Matter Mater. Phys.* **2008**, *77*, 235424.
(65) Finazzi, E.; Di Valentin, C.; Pacchioni, G.; Selloni, A. *J. Chem. Phys.* **2008**, *129*, 154113.
(66) Mattioli, G.; Filippone, F.; Alippi, P.; Amore Bonapasta, A. *Phys. Rev. B: Condens. Matter Mater. Phys.* **2008**, *78*, 241201.
(67) Morgan, B. J.; Watson, G. W. *Surf. Sci.* **2007**, *601*, 5034−5041.
(68) Xu, Z.; Rossmeisl, J.; Kitchin, J. R. *J. Phys. Chem. C* **2015**, *119*, 4827−4833.
(69) Deskins, N. A.; Dupuis, M. *Phys. Rev. B: Condens. Matter Mater. Phys.* **2007**, *75*, 195212.
(70) Wang, L.; Maxisch, T.; Ceder, G. *Phys. Rev. B: Condens. Matter Mater. Phys.* **2006**, *73*, 195107.
(71) García-Mota, M.; Bajdich, M.; Viswanathan, V.; Vojvodic, A.; Bell, A. T.; Nørskov, J. K. *J. Phys. Chem. C* **2012**, *116*, 21077−21082.
(72) Chen, J.; Wu, X.; Selloni, A. *Phys. Rev. B: Condens. Matter Mater. Phys.* **2011**, *83*, 245204.
(73) Dalverny, A.-L.; Filhol, J.-S.; Lemoigno, F.; Doublet, M.-L. *J. Phys. Chem. C* **2010**, *114*, 21750−21756.
(74) Cockayne, E.; Li, L. *Chem. Phys. Lett.* **2012**, *544*, 53−58.
(75) Rollmann, G.; Entel, P.; Rohrbach, A.; Hafner, J. *Phase Transitions* **2005**, *78*, 251−258.
(76) Pinney, N.; Kubicki, J. D.; Middlemiss, D. S.; Grey, C. P.; Morgan, D. *Chem. Mater.* **2009**, *21*, 5727−5742.
(77) Lodziana, Z. *Phys. Rev. Lett.* **2007**, *99*, 206402.
(78) Santos-Carballal, D.; Roldan, A.; Grau-Crespo, R.; de Leeuw, N. H. *Phys. Chem. Chem. Phys.* **2014**, *16*, 21082−21097.
(79) Agarwal, V.; Metiu, H. *J. Phys. Chem. C* **2016**, *120*, 19252−19264.
(80) Ding, H.; Lin, H.; Sadigh, B.; Zhou, F.; Ozoliņš, V.; Asta, M. *J. Phys. Chem. C* **2014**, *118*, 15565−15572.
(81) Coquet, R.; Willock, D. J. *Phys. Chem. Chem. Phys.* **2005**, *7*, 3819.
(82) Kresse, G.; Furthmuller, J. *Phys. Rev. B: Condens. Matter Mater. Phys.* **1996**, *54*, 11169−11186.
(83) Kresse, G.; Furthmüller, J. *Comput. Mater. Sci.* **1996**, *6*, 15−50.
(84) Perdew, J. P.; Burke, K.; Ernzerhof, M. *Phys. Rev. Lett.* **1996**, *77*, 3865−3868.
(85) Blöchl, P. E. *Phys. Rev. B: Condens. Matter Mater. Phys.* **1994**, *50*, 17953−17979.
(86) Krukau, A. V.; Vydrov, O. A.; Izmaylov, A. F.; Scuseria, G. E. *J. Chem. Phys.* **2006**, *125*, 224106.
(87) McCabe, R.; Trovarelli, A. *Appl. Catal., B.* **2016**, in press. Available at the following: http://dx.doi.org/10.1016/j.apcatb.2016.04.044.
(88) Azimi, G.; Dhiman, R.; Kwon, H.-M.; Paxson, A. T.; Varanasi, K. K. *Nat. Mater.* **2013**, *12*, 315−320.
(89) Carchini, G.; García-Melchor, M.; Łodziana, Z.; López, N. *ACS Appl. Mater. Interfaces* **2016**, *8*, 152−160.
(90) Amrute, A. P.; Mondelli, C.; Moser, M.; Novell-Leruth, G.; López, N.; Rosenthal, D.; Farra, R.; Schuster, M. E.; Teschner, D.; Schmidt, T.; Pérez-Ramírez, J. *J. Catal.* **2012**, *286*, 287−297.
(91) Moser, M.; Vilé, G.; Colussi, S.; Krumeich, F.; Teschner, D.; Szentmiklósi, L.; Trovarelli, A.; Pérez-Ramírez, J. *J. Catal.* **2015**, *331*, 128−137.
(92) Vilé, G.; Bridier, B.; Wichert, J.; Pérez-Ramírez, J. *Angew. Chem., Int. Ed.* **2012**, *51*, 8620−8623.
(93) Vilé, G.; Colussi, S.; Krumeich, F.; Trovarelli, A.; Pérez-Ramírez, J. *Angew. Chem., Int. Ed.* **2014**, *53*, 12069−12072.
(94) García-Melchor, M.; Bellarosa, L.; López, N. *ACS Catal.* **2014**, *4*, 4015−4020.
(95) García-Melchor, M.; López, N. *J. Phys. Chem. C* **2014**, *118*, 10921−10926.
(96) Haider, M. H.; Dummer, N. F.; Knight, D. W.; Jenkins, R. L.; Howard, M.; Moulijn, J.; Taylor, S. H.; Hutchings, G. J. *Nat. Chem.* **2015**, *7*, 1028−1032.
(97) Qiao, Z.-A.; Wu, Z.; Dai, S. *ChemSusChem* **2013**, *6*, 1821−1833.
(98) Bruix, A.; Neyman, K. M. *Catal. Lett.* **2016**, *146*, 2053−2080.
(99) Lin, Y.; Wu, Z.; Wen, J.; Poeppelmeier, K. R.; Marks, L. D. *Nano Lett.* **2014**, *14*, 191−196.
(100) Capdevila-Cortada, M.; López, N. *Nature Mater.* **2016**, DOI: 10.1038/nmat4804.
(101) Zhou, J.; Mullins, D. R. *Surf. Sci.* **2006**, *600*, 1540−1546.
(102) Mullins, D. R.; Robbins, M. D.; Zhou, J. *Surf. Sci.* **2006**, *600*, 1547−1558.
(103) Albrecht, P. M.; Mullins, D. R. *Langmuir* **2013**, *29*, 4559−4567.
(104) Bennett, L. J.; Jones, G. *Phys. Chem. Chem. Phys.* **2014**, *16*, 21032−21038.
(105) Kulik, H. J.; Marzari, N. *J. Chem. Phys.* **2011**, *135*, 194105.
(106) Janesko, B. G.; Henderson, T. M.; Scuseria, G. E. *Phys. Chem. Chem. Phys.* **2009**, *11*, 443−454.
(107) Henderson, T. M.; Paier, J.; Scuseria, G. E. *Phys. Status Solidi B* **2011**, *248*, 767−774.
(108) Freysoldt, C.; Grabowski, B.; Hickel, T.; Neugebauer, J.; Kresse, G.; Janotti, A.; Van de Walle, C. G. *Rev. Mod. Phys.* **2014**, *86*, 253−305.
(109) Wang, Y.; Cheng, H.-P. *J. Phys. Chem. C* **2013**, *117*, 2106−2112.
(110) Hsu, H.; Umemoto, K.; Cococcioni, M.; Wentzcovitch, R. *Phys. Rev. B: Condens. Matter Mater. Phys.* **2009**, *79*, 125124.
(111) Kropp, T.; Paier, J.; Sauer, J. *J. Am. Chem. Soc.* **2014**, *136*, 14616−14625.
(112) Wu, X.-P.; Gong, X.-Q. *J. Am. Chem. Soc.* **2015**, *137*, 13228−13231.
(113) Qiao, B.; Wang, A.; Yang, X.; Allard, L. F.; Jiang, Z.; Cui, Y.; Liu, J.; Li, J.; Zhang, T. *Nat. Chem.* **2011**, *3*, 634−641.
(114) Fu, Q.; Saltsburg, H.; Flytzani-Stephanopoulos, M. *Science* **2003**, *301*, 935−938.
(115) Rollmann, G.; Rohrbach, A.; Entel, P.; Hafner, J. *Phys. Rev. B: Condens. Matter Mater. Phys.* **2004**, *69*, 165107.
(116) Scanlon, D. O.; Dunnill, C. W.; Buckeridge, J.; Shevlin, S. A.; Logsdail, A. J.; Woodley, S. M.; Catlow, C. R. A.; Powell, M. J.; Palgrave, R. G.; Parkin, I. P.; Watson, G. W.; Keal, T. W.; Sherwood, P.; Walsh, A.; Sokol, A. A. *Nat. Mater.* **2013**, *12*, 798−801.
(117) El-Sayed, A.; Borghetti, P.; Goiri, E.; Rogero, C.; Floreano, L.; Lovat, G.; Mowbray, D. J.; Cabellos, J. L.; Wakayama, Y.; Rubio, A.; Ortega, J. E.; de Oteyza, D. G. *ACS Nano* **2013**, *7*, 6914−6920.
(118) Selcuk, S.; Selloni, A. *Nat. Mater.* **2016**, *15*, 1107−1112.
(119) García-Mota, M.; Vojvodic, A.; Metiu, H.; Man, I. C.; Su, H.-Y.; Rossmeisl, J.; Nørskov, J. K. *ChemCatChem* **2011**, *3*, 1607−1611.
(120) García-Melchor, M.; Vilella, L.; López, N.; Vojvodic, A. *ChemCatChem* **2016**, *8*, 1792−1798.
(121) Bajdich, M.; García-Mota, M.; Vojvodic, A.; Nørskov, J. K.; Bell, A. T. *J. Am. Chem. Soc.* **2013**, *135*, 13521−13530.
(122) Hall, D. E. *J. Electrochem. Soc.* **1983**, *130*, 317.
(123) Lyons, M. E. G.; Brandon, M. P. *Int. J. Electrochem. Sci.* **2008**, *3*, 1386−1424.
(124) Bediako, D. K.; Lassalle-Kaiser, B.; Surendranath, Y.; Yano, J.; Yachandra, V. K.; Nocera, D. G. *J. Am. Chem. Soc.* **2012**, *134*, 6801−6809.
(125) Görlin, M.; Chernev, P.; Ferreira de Araújo, J.; Reier, T.; Dresp, S.; Paul, B.; Krähnert, R.; Dau, H.; Strasser, P. *J. Am. Chem. Soc.* **2016**, *138*, 5603−5614.
(126) Dionigi, F.; Strasser, P. *Adv. Energy Mater.* **2016**, 1600621.

(127) Hegner, F.; Galan-Mascaros, J.; López, N., *in press*.
(128) Nie, P.; Shen, L.; Luo, H.; Ding, B.; Xu, G.; Wang, J.; Zhang, X. *J. Mater. Chem. A* **2014**, *2*, 5852−5857.
(129) Emery, A. A.; Saal, J. E.; Kirklin, S.; Hegde, V. I.; Wolverton, C. *Chem. Mater.* **2016**, *28*, 5621−5634.
(130) Körbel, S.; Marques, M. A. L.; Botti, S. *J. Mater. Chem. C* **2016**, *4*, 3157−3167.